



Flavour physics and CP violation / Physique de la saveur et violation de CP

Future flavour physics experiments: LHCb and Super B factories

Futures expériences sur la physique de la saveur : LHCb et super-usines à B

Marie-Hélène Schune, Achille Stocchi *

Laboratoire de l'accélérateur linéaire, IN2P3-CNRS et université de Paris-Sud, BP 34, 91898 Orsay cedex, France

ARTICLE INFO

Article history:

Available online 4 January 2012

Keywords:

Flavour physics
LHCb
Super B factories

Mots-clés:

Physique de la saveur
LHCb
Super usine à B

ABSTRACT

In this article we present the physics programs for LHCb and for an e^+e^- high luminosity asymmetric B factory. Using a few examples, we will show how the measurements which can be performed will allow us to study, in a unique manner, the structure of the New Physics beyond the Standard Model, if discovered at LHC with the general purpose detectors ATLAS and CMS, and/or eventually to extend the domain of the New Physics search to larger energy not accessible at LHC.

© 2011 Published by Elsevier Masson SAS on behalf of Académie des sciences.

RÉSUMÉ

Dans cet article nous présentons le programme de physique de LHCb et celui d'une future usine à B asymétriques e^+e^- à haute luminosité. En utilisant quelques exemples nous montrerons comment les mesures qui seront effectuées permettront d'étudier la structure de la nouvelle physique au delà du Modèle Standard si elle est mise en évidence par les expériences ATLAS et CMS au LHC, et/ou d'étendre le domaine de la recherche de la nouvelle physique à des énergies plus élevées et non accessibles au LHC.

© 2011 Published by Elsevier Masson SAS on behalf of Académie des sciences.

1. The LHCb experiment

1.1. Introduction

The LHCb experiment has been conceived to study CP violation and other rare phenomena in B hadron decays with very high precision. It runs at the CERN Large Hadron Collider (LHC). The LHC is a two-ring-superconducting-hadron accelerator and collider installed in the existing 27 km tunnel that was constructed for the CERN LEP machine. At the LHC, bunches of protons collide every 25 ns in four interaction regions. The LHCb experiment is installed in one of these crossing-points. The LHCb detector is a single-arm spectrometer with a forward angular coverage from approximately 10 mrad to 300 mrad. The choice of the detector geometry is motivated by the fact that in proton–proton collisions at high energies both the b and \bar{b} quarks are predominately produced in the same forward or backward cone. There is a planned upgrade [1] of the LHCb detector which involves at least five years of operating at about $2 \times 10^{33} \text{ cm}^{-2} \text{ s}^{-1}$. The aim is to collect a data sample of $\sim 100 \text{ fb}^{-1}$, as well as to increase the trigger efficiency for hadronic decays by at least a factor of two.

In the following part, we will try to present some of the main physics expectations for the LHCb experiment, focusing on the foreseen measurements which are specific to LHCb. This peculiarity could be due to the very large statistics which soon

* Corresponding author.

E-mail addresses: schunem@lal.in2p3.fr (M.-H. Schune), stocchi@lal.in2p3.fr (A. Stocchi).

should be available or to the study of B_s mesons which are not produced at (super) B -factories. Some choices have thus been made and one should keep in mind that a large part of LHCb physics could not be described here (e.g. charm physics). Since LHCb is now taking data, a special care is given to present the current performance; however, one should keep in mind that the current results are not yet the final ones and some improvements in yields or resolutions are expected.

1.2. Detector

The LHCb detector, which is primarily meant to measure CP violating and rare decays of hadrons containing b and c quarks, is a single-arm magnetic dipole spectrometer with a polar angular coverage with respect to the beam line of approximately 15 to 300 mrad in the horizontal bending plane, and 15 to 250 mrad in the vertical non-bending plane. The detector is described in detail elsewhere [2]. Since the beginning of data taking (2009), all subdetectors are fully operational and in a stable condition. The detector elements are placed along the beam line of the LHC starting with the Vertex Locator, a silicon strip device that surrounds the proton–proton interaction region and is positioned 8 mm from the beam during collisions. It provides precise locations for primary proton–proton interaction vertices, the locations of decays of long lived hadrons, and contributes to the measurement of track momenta. Other detectors used to measure track momenta comprise a large area silicon strip detector located before a 3.7 Tm dipole magnet, and a combination of silicon strip detectors and straw drift chambers placed afterward. Two Ring Imaging Cherenkov (RICH) detectors are used to identify charged hadrons. Further downstream an Electromagnetic Calorimeter (ECAL) is used for photon detection and electron identification, followed by a Hadron Calorimeter (HCAL), and a system consisting of alternating layers of iron and gaseous chambers that distinguishes muons from hadrons (MUON). The ECAL, MUON, and HCAL provide the capability of first-level hardware triggering.

1.3. Operational considerations

Since March 2010, the LHCb experiment has been successfully taking data: at the end of 2010 an integrated luminosity of about 35 pb^{-1} has been recorded with a data taking efficiency exceeding 90%. The year 2011 is also extremely successful: about 750 pb^{-1} have already been registered and 1 fb^{-1} is expected for the end of the year. However, the running conditions are not exactly those foreseen [3]: the centre of mass energy is equal to 7 TeV instead of 14 TeV, and LHCb routinely runs at an instantaneous luminosity of $3.5 \times 10^{32} \text{ cm}^{-2} \text{ s}^{-1}$ (more than 1.5 times the design value).

The consequence of the smaller centre of mass energy is mainly a reduced value for the $b\bar{b}$ cross section by about a factor 2. Some of the first LHCb results are related to this parameter of prime importance for the b -physics program of LHCb: the $b\bar{b}$ cross section has been measured both using B hadrons semi-leptonic decays and $B \rightarrow J/\psi X$ decays, getting, respectively, $298 \pm 15 \pm 43 \text{ } \mu\text{barn}$ [4] and $295 \pm 4 \pm 48 \text{ } \mu\text{barn}$ [5] in 4π acceptance. These values are fully consistent with the cross section of $500 \text{ } \mu\text{barn}$ at 14 TeV of energy in the centre of mass system used in [3]. As already stated, the beam conditions were not those designed for LHCb, and this has some impact on the data taking. The number of proton bunches in the LHC is lower than the design value, however, due to stronger focussing of the beams, an instantaneous luminosity of $3.5 \times 10^{32} \text{ cm}^{-2} \text{ s}^{-1}$ is obtained. This implies that the number of collisions per crossing is larger by a factor 2 to 3 than the LHCb design. These running conditions have several consequences on the data taking: the trigger, which is highly configurable, evolved a lot to match the exponential increase of the LHC luminosity and the physics requirements in 2010. In particular, the choice was made to preserve the muon triggers which are of prime importance for the first physics goals of the LHCb experiment, while the hadronic and electromagnetic trigger thresholds had to be increased during the year in order to cope with the operational conditions. In 2011, due to the higher number of proton bunches, the running conditions were easier.

1.4. Search for the $B_s \rightarrow \mu^+ \mu^-$ decay mode

The measurement of the Branching Ratio (BR) of this decay mode is a probe to the mass and couplings of a potential physics beyond Standard Model (SM). Indeed, the BR for this decay is expected to be extremely small due to the helicity and loop (Flavour-Changing Neutral Current) suppression. The SM prediction is $(3.35 \pm 0.32) \times 10^{-9}$ [6]. Contributions from new particles from Beyond Standard Model (BSM) models, such as, for example, supersymmetry, could enhance the BR up to 100 times. The best limit before LHCb startup was achieved by the CDF experiment: $\text{BR} < 4.3 \times 10^{-8}$ at 95% CL [7]. The LHCb experiment is well suited for studying this decay due to a high trigger efficiency, a good muon identification and an excellent invariant mass resolution. The analysis [8] is based on two variables: the $\mu^+ \mu^-$ invariant mass and the output of a multivariate analysis discriminant (Boosted Decision Tree) using geometrical and kinematical information of the decay (impact parameter significance of the muons, B_s proper time, impact parameter of the B_s , distance of closest approach between the two muons, muon isolation). The likelihood functions of these two variables are calibrated on real data using control channels. The two-dimensional space defined by these variables is divided into bins. The distribution of the invariant mass in the four Boosted Decision Tree (BDT) bins is shown in Fig. 1. The observed events are in good agreement not only with background expectations but also with the presence of signal according to SM predictions. The compatibility of the distribution of events in the invariant mass versus BDT plane with a given branching ratio hypothesis is evaluated using the CL_s method [9]. This provides two estimators: CL_s is a measure of the compatibility of the observed distribution with

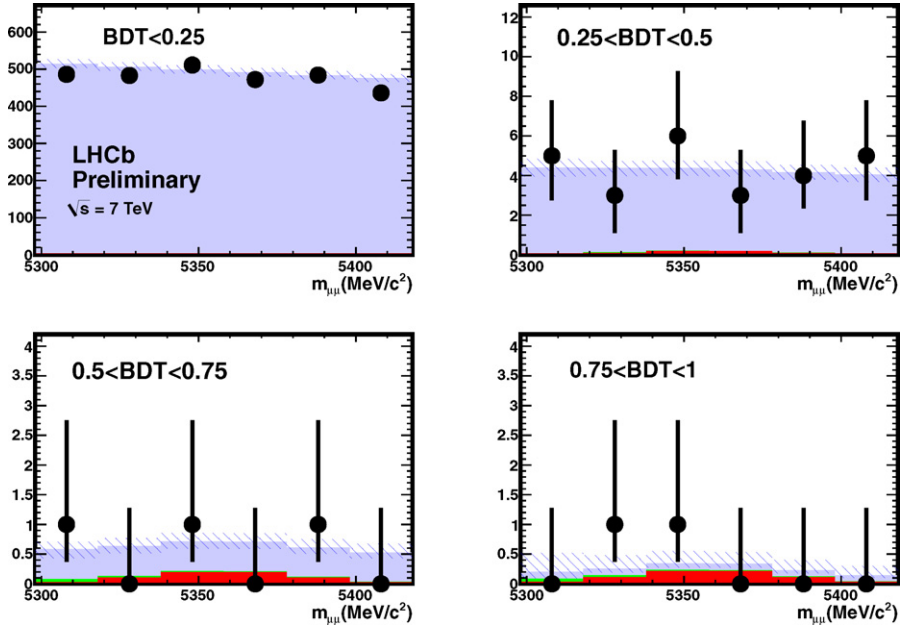


Fig. 1. $B_s \rightarrow \mu^+ \mu^-$: distribution of selected dimuon events in the distribution of selected dimuon events in the invariant mass plane for the four BDT bins. The black dots are data, the light blue histogram shows the contribution of the combinatorial background with its uncertainty (hatched area), the green histogram shows the contribution of the $B_{(s)} \rightarrow h^+ h^-$ background and the red filled histogram shows the contribution of $B_s \rightarrow \mu^+ \mu^-$ signal events according to the SM rate. The uncertainty on data in the first BDT bin is smaller than the size of the dots.

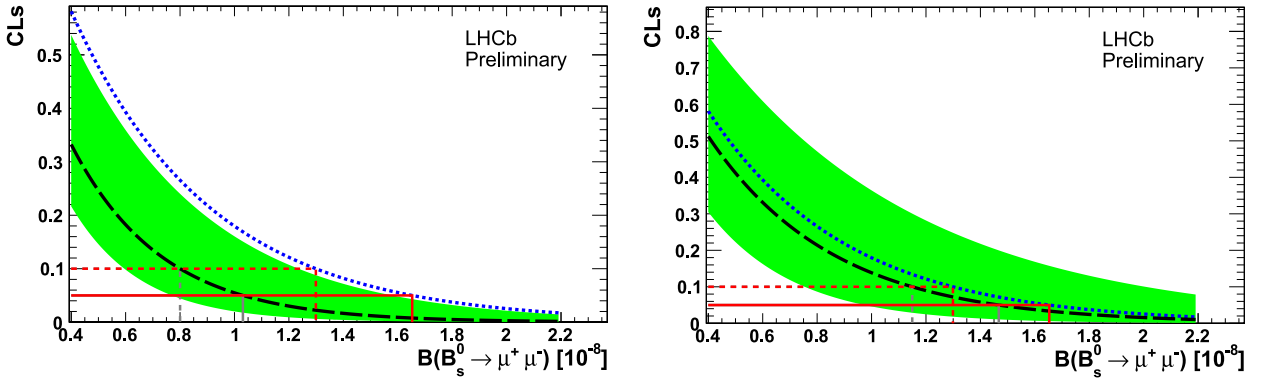


Fig. 2. $B_s \rightarrow \mu^+ \mu^-$: expected distributions of possible values of CL_s (dashed black line) under the hypothesis to observe background only (left) and under the hypothesis to observe a combination of background and signal events according to the SM rate (right). On both graphs, the green areas cover the region of $\pm 1\sigma$ of compatible observations. The observed distributions of CL_s as a function of the assumed branching ratio are shown as dotted blue lines. The measured upper limits at 90% and 95% CL are also shown.

the signal hypothesis, while CL_b is a measure of the compatibility with the background-only hypothesis. The distributions of expected CL_s values are shown as dashed (black) lines in Fig. 2 under the hypotheses to observe background events only (left) or a combination of background plus SM events (right). The green shaded areas cover the region of $\pm 1\sigma$ of compatible observations. The observed CL_s as a function of the assumed branching ratio is shown as dotted (blue) line. The obtained limit is $BR < 1.5 \times 10^{-8}$ at 95% CL, which is still more than a factor 4 above the value predicted by the SM.

1.5. Study of the $B_d \rightarrow K^* \mu^+ \mu^-$ decay mode

Decays generated by the FCNC, such as $B \rightarrow K^* \mu^+ \mu^-$ are also very interesting to probe BSM physics. The diagrams contributing to this decay mode are shown in Fig. 3. The Operator Product Expansion allows one to parameterise the process in terms of an effective Hamiltonian:

$$H_{\text{eff}} = -\frac{4G_F}{\sqrt{2}} V_{tb} V_{ts}^* \sum_{i=1}^{10} [C_i(\mu) O_i(\mu) + C'_i(\mu) O'_i(\mu)] \quad (1)$$

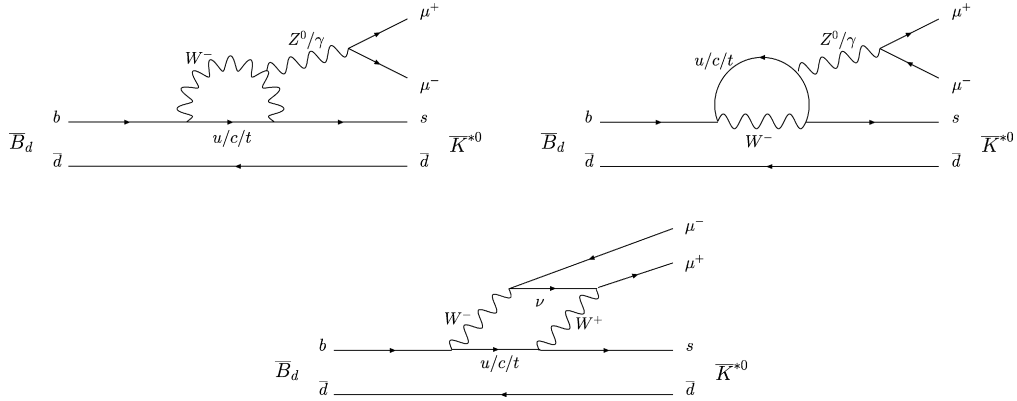


Fig. 3. The Standard Model Feynman diagrams for the decay $B \rightarrow K^* \mu^+ \mu^-$.

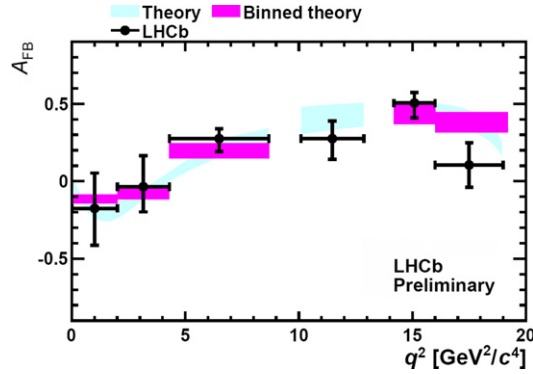


Fig. 4. A_{FB} distribution as a function of the square of the $\mu^+ \mu^-$ invariant mass. The theory predictions are described from [14].

where V_{tb} and V_{ts} are the numerically dominant CKM factors and, following the conventions of Ref. [10], primes (no primes) denote right-handed (left-handed) contributions. The local operators $O_i(\mu)$ describe the long range contributions to the decay, while the Wilson coefficients $C_i(\mu)$ describe the short range contributions calculable perturbatively. The parameter μ is the renormalisation scale where the two quantities are matched and typically this is $\mathcal{O}(m_b)$. For the $B \rightarrow K^* \mu^+ \mu^-$ decay mode the $i = 7, 9$ and 10 operators are the dominating ones (the right-handed ones are heavily suppressed). Among the observables which can be built, the Forward-Backward asymmetry A_{FB} in the $\mu^+ \mu^-$ rest frame as a function of the $\mu^+ \mu^-$ invariant mass is of interest, and in particular the invariant mass value, s_0 , where A_{FB} crosses zero. The value s_0 can be precisely predicted by the SM and BSM physics could give a sizeable deviation to this prediction. The position of s_0 depends on the values and signs of C_7 , C_9 and C_{10} . Some first measurements have been conducted at B factories and Tevatron [11], but are statistically limited. LHCb is expected to collect 7200 events for 2 fb^{-1} with a background over signal ratio around 0.2; to be compared with the 450 events expected from the Belle and BABAR experiments together. By fitting a linear function to A_{FB} around the zero crossing region, a precision on s_0 of 0.46 GeV^2 with 2 fb^{-1} of data and a $b\bar{b}$ cross section of $500 \mu\text{barn}$ is foreseen [3]. In addition, with large statistics, using the whole set of angular observables, LHCb can measure [12] the transversity amplitudes as a function of the dimuon mass [10]. The two crucial points for the study of the angular distributions of the decay products of the $B \rightarrow K^* \mu^+ \mu^-$ decay mode are the understanding of the event acceptance as a function of the whole set of angular variables and of their distributions for the background.

With 300 pb^{-1} of data, LHCb has already been able to measure the Forward-Backward asymmetry A_{FB} as a function of the square of the $\mu^+ \mu^-$ invariant mass with a better precision than the previous experiment (B factories and Tevatron) [13]. The A_{FB} distribution is shown in Fig. 4 and, with the current level of statistics, there is a good agreement between theory and experiment.

1.6. Study of the photon polarisation

The SM predicts a right-handed component in the photons generated by the $b \rightarrow s \gamma$ transitions suppressed by a term $\mathcal{O}(m_s/m_b)$ due to the $V-A$ coupling of the W boson. In several extensions of the SM, the photon can acquire an appreciable right-handed component due to chirality flip in the transition [15] with a departure from the SM value of the branching ratio. The measurement of the photon polarisation is thus a way to test the Lorentz structure of a potential contribution of physics beyond the SM.

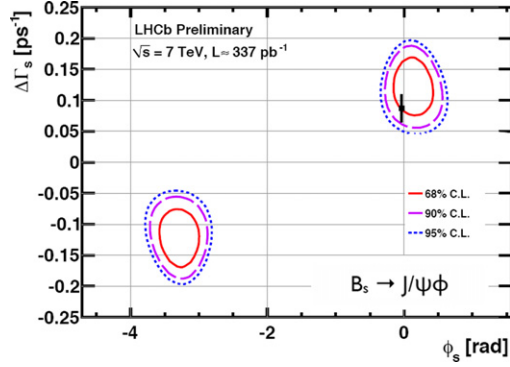


Fig. 5. 2D likelihood confidence regions in the ϕ_s - $\Delta\Gamma_s$ plane for the $B_s \rightarrow J/\psi\phi$ analysis. The second solution at $\pi-\phi_s, -\Delta\Gamma_s$ is unavoidable with this decay mode and due to the structure of the equations describing the B_s and \bar{B}_s time evolution. The black point corresponds to the theoretical predicted SM value.

One experimental technique to probe the photon helicity is via mixing-induced CP asymmetries [16]. The combination of the Belle and BABAR measurements of the time-dependent CP asymmetry using the $B \rightarrow (K_s^0\pi^0)\gamma$ decay mode [17] leads to an uncertainty of ~ 0.16 on the fraction of wrongly polarised photon. A similar study can be made using the $B_s \rightarrow \phi\gamma$ decay mode. For the B_s system the decay width difference between the two weak eigenstates, $\Delta\Gamma_s$, cannot be neglected in the proper-time distribution. The time evolution of the $B_s \rightarrow \phi\gamma$ decay rare is given by:

$$\frac{d\Gamma(B_s \rightarrow \phi\gamma)}{dt} \propto e^{-\Gamma_s t} \left(\cosh \frac{\Delta\Gamma_s t}{2} - \sin 2\Psi \cos \phi_s \sinh \frac{\Delta\Gamma_s t}{2} \right) \quad (2)$$

where $\tan \Psi = \left| \frac{\bar{B}_s \rightarrow \phi\gamma_R}{B_s \rightarrow \phi\gamma_L} \right|$ is the ratio of the decay amplitudes and $\cos \phi_s \sim 1$ in the SM. A signal sample of 11 000 events for 2 fb^{-1} and a $b\bar{b}$ cross section of $500 \mu\text{barn}$ with a background over signal ratio smaller than 0.9 at 90% CL is expected [3]. This should allow us to measure $\sin 2\Psi$ with a 20% statistical uncertainty and thus $\left| \frac{\bar{B}_s \rightarrow \phi\gamma_R}{B_s \rightarrow \phi\gamma_L} \right|$ with a precision of the order of 0.1. The crucial point of this analysis is to understand the proper-time acceptance.

Another decay mode which would allow us to test the photon helicity is the $B \rightarrow K^*e^+e^-$ decay mode. Compared to the $B \rightarrow K^*\mu^+\mu^-$ decay mode, it has a much better sensitivity to the photon polarisation due to the small electron mass [18]. With a signal sample of about 200 events for an integrated luminosity of 2 fb^{-1} , a $b\bar{b}$ cross section of $500 \mu\text{barn}$ and a background over signal ratio of the order of 1, the expected statistical accuracy on the fraction of wrongly polarised photons is of the order of 0.1 [19]. This analysis is limited by the statistics and will benefit from the LHCb upgrade.

1.7. Measurement of the ϕ_s angle using the $B_s \rightarrow J/\psi\phi$ decay mode

For a final state f equal to its CP conjugate ($f = \bar{f}$), a CP violating phase arises from the interference between B_s decay to f either directly or via B_s - \bar{B}_s oscillations, producing a difference in the proper-time distributions of B_s mesons and \bar{B}_s mesons. Within the SM this decay is dominated by $\bar{b} \rightarrow \bar{c}c\bar{s}$ quark level transitions, neglecting QCD penguin contribution the phase is: $\phi_s = -2\beta_s$, where $\beta_s = \arg(-V_{ts}V_{tb}^*/V_{cs}V_{cb}^*)$. In the SM this mixing phase is very small: $\phi_s \sim 0.04$ but it can receive sizeable new physics contributions through box diagrams. This measurement is thus a way to probe new physics couplings. Even if conceptually this analysis is similar to the famous $\sin 2\beta$ measurement performed at B factories, it is more challenging not only because of the fast B_s oscillation but also because the final state involves two vector mesons and thus a full angular analysis has to be performed. The measurement of the ϕ_s angle requires then a time-dependent, flavour-tagged, angular analysis of the decay rates. The result of this analysis is shown in Fig. 5 in the ϕ_s - $\Delta\Gamma_s$ plane. Another way to perform this measurement is to use the $B_s \rightarrow J/\psi f_0$ decay mode, thus avoiding the angular analysis complication. Using an integrated luminosity of 300 pb^{-1} of data, these two analyses have been performed [20] and ϕ_s is measured with a precision better than that from the Tevatron [21]: $\phi_s = 0.03 \pm 0.16 \pm 0.07 \text{ rad}$. In all cases, even with an integrated luminosity of 10 fb^{-1} , the measurement should be still statistically limited and will thus benefit from the upgrade plans.

1.8. Measurement of the γ angle of the unitarity triangle

The γ angle of the CKM matrix is the least well constrained of the angles of the unitarity triangle (see for example Fig. 6). Many different channels can be used. They are not only different from an analysis point of view, but they also differ from the type of diagrams involved: the decays due to tree diagrams can be seen as Standard Model candles, while those where penguin diagrams play a role are, in principle, sensitive to new physics contributions. The decay $B_s \rightarrow D_s^\pm K^\mp$ and its charge conjugate can proceed through two tree-decay diagrams, the interference of which gives access to the phase γ if the B_s mixing phase is determined otherwise (e.g. with the $B_s \rightarrow J/\psi\phi$ decay mode). Another large family of decays which will

allow one to precisely measure γ is $B_d \rightarrow DK^{(*)}$. Finally, the family of decays which consists in a pair of charged hadrons h^+h^- (h is a pion or a kaon) of both B_d and B_s mesons, have decay rates with non-negligible contributions from penguin diagrams, making them sensitive to BSM physics. The dependence on γ comes from CP time-dependent measurements from $B_d \rightarrow \pi^+\pi^-$ and $B_s \rightarrow K^+K^-$ which allow to extract γ relying on U-Spin symmetry [22]. For all those decays, the key ingredients are the powerful particle identification from the RICH detectors and a very good mass resolution. One can estimate that the LHCb achievable precision on γ will be of the order of 7 degrees with 2011 data. With the LHCb upgrade and an integrated luminosity of 100 fb^{-1} , one will be able to compare precisely the γ measurements obtained from pure tree diagrams where no BSM physics contributions are expected and the one obtained from charmless B decays where penguin diagrams play a role and thus new particles can contribute.

2. The future Super B factories

The current generation of asymmetric B factory experiments, BABAR at PEP-II and Belle at KEKB have shown that a variety of measurements can be performed in a clean environment. In addition most of the golden modes (as described in this issue by Adrian Bevan [23] and Antony Sanda [24]) are not limited by systematics, and thus the precision could be improved if a large data sample is collected.

In this section we present the physics program of a next generation of asymmetric B factory collecting an integrated luminosity of 50 to 100 ab^{-1} . A reasonable benchmark for obtaining such a data sample is of the order of five years of running. Meeting both constraints requires a collider luminosity of $10^{36} \text{ cm}^{-2} \text{ s}^{-1}$ or more, yielding $15 \text{ ab}^{-1}/\text{year}$ (a year is supposed to effectively count 1.5×10^7 seconds). Reaching this luminosity with a collider design extrapolated from PEP-II or KEKB, is difficult; beam currents and thus power consumption are very high, and the detector backgrounds difficult to sustain. The low emittance crabbed waist design of SuperB provides a solution to the problem, allowing us to reach the needed luminosity with beam currents and power consumption similar to those at PEP-II. Following the success of the test of the crab waist concept at Frascati [25] two projects actually exist based on these new concepts: SuperB (to be built in Italy near Frascati) and SuperKEKB (which will be based at KEK). The two projects have been recently approved and, for both projects, the construction will start current 2012. Six years will be then necessary to start the data taking.

In the following we show the potentiality of the best possible future Super B factory (called SuperB in the following), collecting 75 ab^{-1} , with at least one longitudinal polarised beam and with the possibility of running at different threshold energies and, in particular, at the charm threshold (the $\psi(3770)$ resonance). The physics program for a high luminosity Super B factory is described in detail in several publications (see for instance [26]).

Since SuperB will take data in the LHC era, it is reasonable to ask how the physics reach compares with the B physics potential of the LHC experiments, most notably LHCb, which has been presented in the previous section. We dedicate a section to this comparison.

2.1. The physics program

2.1.1. Future metrology of the CKM matrix

One lesson from the B factories is that precision is crucial for testing the SM in the flavour sector, performing redundant measurements of the same underlying quantity. In Fig. 6 we show the regions on the $\bar{\rho}-\bar{\eta}$ plane selected by different constraints assuming the current measurement precision (left), and that expected at SuperB (right). It is important to note that for achieving that, several measurements have to be performed at the % level; among them we mention the three Unitarity Triangle (UT) angles (α , β and γ) and the elements $|V_{ub}|$ and $|V_{cb}|$ measured through semileptonic B decays. For the latter it is of crucial importance to achieve the improvements of the Lattice calculations as described in (Damir Bečirević and Vittorio Lubicz, this issue [27]). These measurements could allow tests of the consistency of the Standard Model at a few per mille level. The inconsistency of the different constraints, such as that shown in Fig. 6 (right), will be a clear indication of New Physics beyond the Standard Model.

2.1.2. The New Physics sensitive measurements in the B sector

In this section we highlight the golden channels for SuperB. In fact, at SuperB, a golden channel is any channel that can be calculated in the Standard Model with a very small theoretical error. SuperB will be able to measure many rare decay processes that are sensitive to different NP scenarios. An extensive discussion is given in [26]. It is worthwhile to mention the measurements of the branching fractions of several rare decays as: $Br(B \rightarrow X_s \gamma)$, $Br(B \rightarrow \tau \nu)$, $Br(B \rightarrow X_s \ell \ell)$, $Br(B \rightarrow K \nu \bar{\nu})$, and of related direct and indirect CP asymmetries as $A_{CP}(B \rightarrow X_s \gamma)$, $S_{K_s \pi^0 \gamma}$ and of the entire set of $b \rightarrow s$ penguin-dominated non-leptonic modes.

It has to be noted that most of the golden channels are very challenging from an experimental point of view. One of the main characteristics of the SuperB physics program is the possibility of performing inclusive measurements, which are often better under control from theoretical point of view, in addition to exclusive ones; and in addition the possibility of measuring channels with neutrinos, γ , K_L , ... in the final states.

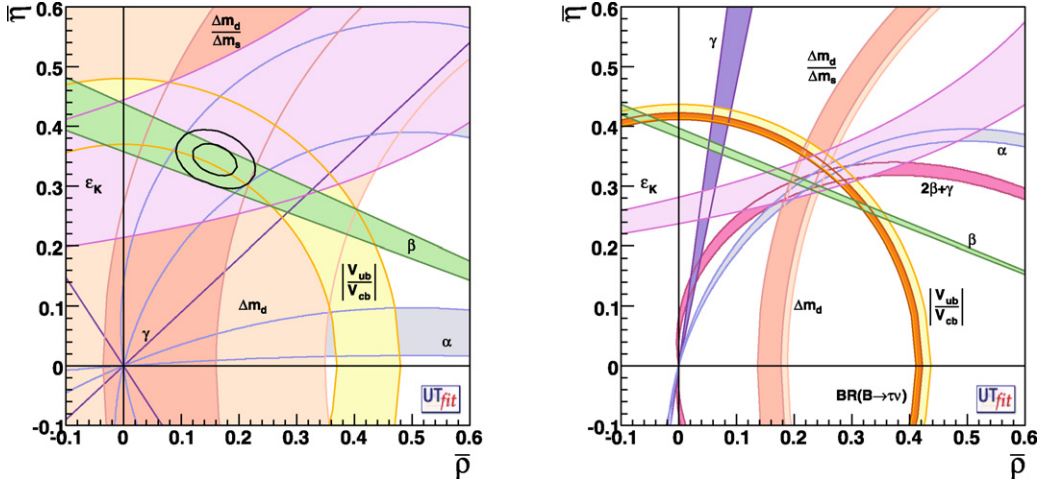


Fig. 6. Regions corresponding to 95% probability for $\bar{\rho}$ and $\bar{\eta}$ selected by different constraints, assuming present central values with present errors (left) or the same central values with errors expected at SuperB (right).

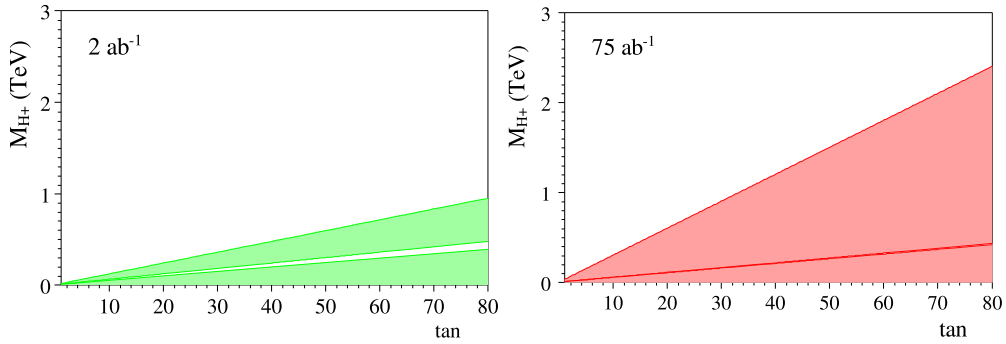


Fig. 7. Exclusion regions in the $m(H^+)$ – $\tan\beta$ plane arising from the combinations of the measurement of $Br(B \rightarrow \tau\nu)$ and $Br(B \rightarrow \mu\nu)$ using 2 ab^{-1} (left) and 75 ab^{-1} (right). We assume that the result is consistent with the Standard Model.

In the following we discuss only two examples of the physics reach in two NP scenarios:

Charged Higgs in the high $\tan\beta$ scenario. The precise measurements of the branching fraction $Br(B \rightarrow \ell\nu)$ where $\ell = \mu, \tau$ is a unique probe to constrain NP in the H^+ high $\tan\beta$ scenario ($\tan\beta$ being the ratio of the VEVs of the two Higgs doublets). Fig. 7 shows a comparison of the exclusion plot in the $m(H^+)$ – $\tan\beta$ plane coming from a measurement of $Br(B \rightarrow \tau\nu)$ and $Br(B \rightarrow \mu\nu)$ with different data samples, the presently available 2 ab^{-1} and 75 ab^{-1} , assuming that the result is consistent with the Standard Model.

It is clear that the presence of charged Higgs with mass beyond the TeV could be detected in scenario with high $\tan\beta$.

MSSM with generic squark mass matrices. We now discuss the impact of SuperB on the parameters of the Minimal Supersymmetric Standard Model (MSSM) with generic squark mass matrices parameterised using the mass insertion (MI) approximation [28]. In this framework, the NP flavour-violating couplings are the complex MIs. For simplicity, we consider only the dominant gluino contribution. The relevant parameters are therefore the gluino mass $m_{\tilde{g}}$, the average squark mass $m_{\tilde{q}}$ and the MIs $(\delta_{ij}^d)_{AB}$, where $i, j = 1, 2, 3$ are generation indices and $A, B = L, R$ refer to the helicity of the SUSY partner quarks.

In Fig. 8 we show an example in case of $(\delta_{23}^d)_{LL,LR}$ obtained by requiring that the absolute value of the reconstructed MI is more than 3σ away from zero. From these plots, one can see that SuperB could detect NP effects caused by SUSY masses up to 10–15 TeV, corresponding to $(\delta_{23}^d)_{LL} \sim 1$. Here the relevant constraints come from $B(b \rightarrow s\gamma)$, $A_{CP}(b \rightarrow s\gamma)$, $B(b \rightarrow s\ell^+\ell^-)$, $A_{CP}(b \rightarrow s\ell^+\ell^-)$, Δm_s and A_{SL}^S (the two latter quantities are precisely measured at hadron colliders, Tevatron and LHC).

2.1.3. NP sensitive measurements in the τ sector

Lepton Flavour Violation (LFV) in τ decay is one of the most theoretically and experimentally clean probes to search for NP. This search at SuperB is complementary with the existing neutrino experiments aiming at measuring θ_{13} and the MEG experiment at PSI searching for $\mu \rightarrow e\gamma$. With an integrated luminosity of 75 ab^{-1} SuperB can gain an order of magnitude on several LFV in τ decays (see Table 1), exploring a significant portion of the parameter space of various NP scenarios.

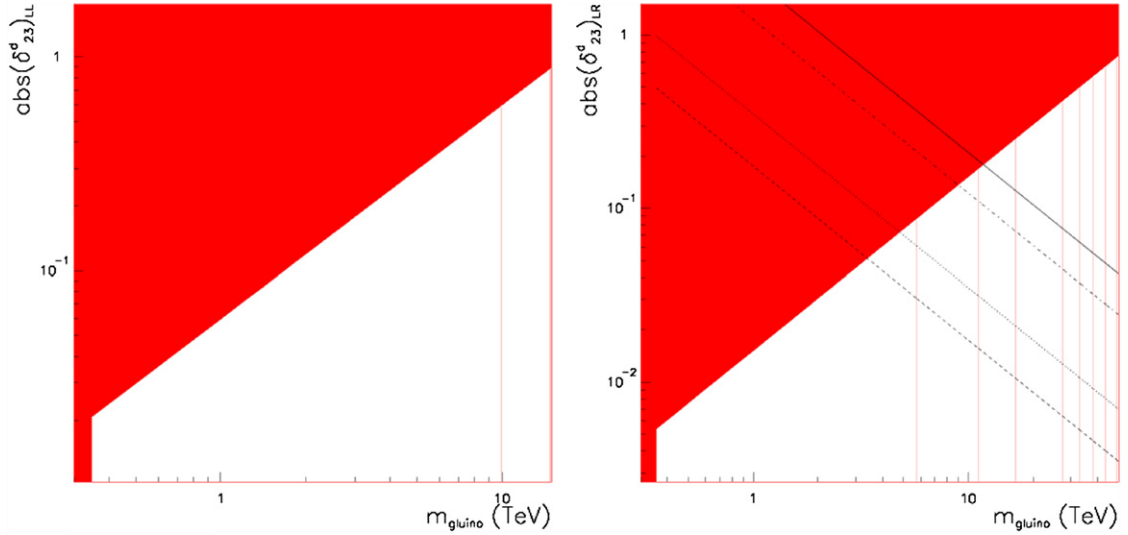


Fig. 8. Sensitivity region of SuperB in the plane $m_{\tilde{g}} - (\delta_{23}^d)_{LL}$ (left) and $m_{\tilde{g}} - (\delta_{23}^d)_{LR}$ (right). The region is obtained by requiring that the reconstructed MI is 3σ away from zero.

Table 1

The experimental sensitivities (in units of 10^{-10}) expected for LFV searches in τ decay.

Final state	$\mu\gamma$	$e\gamma$	3μ	$3e$	$\mu\eta$	$e\eta$	ℓK_S^0
Sensitivity / 10^{-10}	20	20	2	2	4	6	2

A longitudinally-polarised electron beam (at the level of about 85%) is the key to the study of the structure of lepton-flavor-violating couplings in τ decay. Recent studies have shown that the polarisation gives new handles to discriminate between signal and background and thus probably allow to push even further the SuperB sensitivity on LFV measurements. Polarisation opens also the possibility to search for a τ EDM, or for CP violation in τ decay.

2.1.4. Charm physics

Charm physics could play an important role on the NP searches. In fact, among the up-type quarks, only charm allows one to probe for FCNC and thus NP in oscillation phenomena and, in particular, those involving CP violation. It is a unique opportunity since FCNC could be much less suppressed in the up-type than in the down-type quark sectors. It is important to note that in the Standard Model direct CP violation in charm transitions only occur in Cabibbo-suppressed modes at an observable level $\sim O(10^{-3})$ and time-dependent CP asymmetries could reach the 10^{-5} [10^{-4}] level in Cabibbo-allowed and once [doubly]-suppressed modes. The recent observation of $D^0\bar{D}^0$ oscillations, with $x_D, y_D \simeq 0.005$ – 0.01 , has clearly opened the space in which the observation of CP violation could be a manifestation of NP.

SuperB can perform studies on the charm sector in a comprehensive manner, with high luminosity data sample in the $\Upsilon(4S)$ region and also at the $\psi(3770)$ resonance, as the collider is designed to run at lower centre-of-mass energies, at reduced luminosity. With very short low-energy runs, a data sample an order of magnitude greater than that of the final BES-III sample can readily be obtained. Running at the charm threshold should allow one to precisely measure the D decay form factor on semileptonic decays and the decay constant on the leptonic decay. These are important measurements which have to be compared with Lattice QCD calculations. Dalitz analyses of D decays with high statistics could provide inputs to the measurement of the UT angle γ . Finally, FCNC searches are better performed at the charm threshold.

2.1.5. Spectroscopy

The recent results from the B factories provide evidence for the renaissance of hadronic spectroscopy. B factories have discovered new particles at a rate of more than one per year, including the results at lower Υ resonances. SuperB will open a unique window on this physics because it allows a high statistics study in a clean e^+e^- environment ideal for the complicated analyses necessary to pin down the nature of these new hadrons.

The studies of lower Υ resonances would allow tests of extensions of the Standard Model in a manner complementary to the physics program of a classic B factory and to the LHC. Among the possibilities, we mention that to detect the presence of a light pseudoscalar Higgs produced in the decay $\Upsilon(nS) \rightarrow ll\gamma$ ($n = 1, 2, 3$) as an intermediate state (in models like NMSSM) [29].

In addition, the study of $\Upsilon(nS) \rightarrow$ invisible decays allows independent constraints on models with light dark matter (LDM) to be obtained [30].

3. Comparison LHCb SuperB and conclusions

The most striking outcome of any comparison between SuperB and LHCb is that the strengths of the two experiments are largely complementary. For example, the large boost of the B hadrons produced at LHCb allows time-dependent studies of B_s mesons (see the discussion in Sections 1.6, 1.7). Many of the measurements that constitute the primary physics motivation for SuperB cannot be performed in the hadronic environment: for example, modes with missing energy, such as $B^+ \rightarrow \ell^+ \nu_\ell$ and $B^+ \rightarrow K^+ \nu \bar{\nu}$, measurements of the CKM matrix elements $|V_{cb}|$ and $|V_{ub}|$. Conversely, there are key measurements, such as $B_s \rightarrow \mu^+ \mu^-$, $B_s \rightarrow J\psi\phi$ which are unique to the LHCb physics program. NP “discoveries” could come from these measurements in the next two years or so. Where there is overlap in terms of NP reach the channels used are also often complementary. SuperB uses for instance inclusive analyses of processes such as $b \rightarrow s\gamma$ and $b \rightarrow s\ell\ell$ whereas LHCb can perform, earlier in time, similar measurements using exclusive channels. Another example is the measurement of photon polarisation via mixing-induced CP violation in $B^0 \rightarrow K_S^0 \pi^0 \gamma$, which is precluded at LHCb due to the limited capability for channels where the analysis requires that the B decay vertex be determined from a K_S^0 meson. However, measurements of photon polarisation are also accessible to LHCb via $B_s \rightarrow \phi\gamma$ and $B \rightarrow K^* \ell^+ \ell^-$ decay modes.

In the following years flavour physics in the quark sector will be dominated by the LHCb results. This program can be continued running LHCb at higher luminosity improving the precision for some specific and important channels. An $e^+e^- B$ factory at very high luminosity is the next discovery machine, namely the machine needed to push much further the experimental precision to search the new physics in this sector.

References

- [1] The LHCb Collaboration, Expression of interest for an LHCb upgrade, CERN-LHCb-2008-019.
- [2] A. Augusto Alves Jr., et al., LHCb Collaboration, JINST 3 (2008) S08005.
- [3] LHCb Collaboration, B. Adeva, et al., Roadmap for selected key measurements of LHCb, arXiv:0912.4179v2 [hep-ex].
- [4] R. Aaij, et al., LHCb Collaboration, Measurement of $\sigma(pp \rightarrow bbX)$ at $\sqrt{s} = 7$ TeV in the forward region, Phys. Lett. B 694 (2010) 209.
- [5] P. Robbe, Prompt J/ψ and $b \rightarrow J/\psi X$ production in pp collisions, in: Workshop on Discovery Physics at the LHC, Mpumalanga, South Africa, 5–10 December 2010.
- [6] M. Blanke, et al., TUM-HEP-626/06, JHEP 0610 (2006) 003, arXiv:hep-ph/0604057v5.
- [7] CDF Collaboration, CDF Public Note 9892.
- [8] LHCb Collaboration, Search for the rare decay $B_{(s)}^0 \rightarrow \mu^+ \mu^-$ with 300 pb^{-1} at LHCb, LHCb-CONF-2011-037.
- [9] A.L. Read, CERN Yellow Report 2000-005.
- [10] F. Kruger, J. Matias, Probing new physics via the transverse amplitudes of $B \rightarrow K^* \ell^+ \ell^-$ at large recoil, Phys. Rev. D 71 (2005) 094009.
- [11] J.-T. Wei, P. Chang, et al., Belle Collaboration, Phys. Rev. Lett. 103 (2009) 171801, arXiv:0904.0770v2;
B. Aubert, et al., BABAR Collaboration, Phys. Rev. D 79 (2009) 031102, arXiv:0804.4412;
CDF Collaboration, FERMILAB-PUB-11-364-PPD.
- [12] Ulrik Egede, Angular correlations in the $B \rightarrow K^* \mu^+ \mu^-$ decay, LHCb 2007-057.
- [13] LHCb Collaboration, Angular analysis of $B \rightarrow K^* \mu^+ \mu^-$, LHCb-CONF-2011-038.
- [14] C. Bobeth, G. Hiller, D. van Dyk, More benefits of semileptonic rare B decays at low recoil: CP violation, arXiv:1105.0376.
- [15] R.N. Mohapatra, J.C. Pati, Phys. Rev. D 11 (1975) 566;
G. Senjanovic, R.N. Mohapatra, Phys. Rev. D 12 (1975) 1502;
G. Senjanovic, Nucl. Phys. B 153 (1979) 334;
H.E. Haber, G.L. Kane, Phys. Rep. 117 (1985) 75.
- [16] D. Atwood, M. Gronau, A. Soni, Phys. Rev. Lett. (1997) 15, arXiv:hep-ph/9704272.
- [17] <http://www.slac.stanford.edu/xorg/hfag/>.
- [18] Y. Grossman, D. Pirjol, J. High Energy Phys. 0006 (2000) 029.
- [19] Jacques Lefrançois, Marie-Hélène Schune, Measuring the photon polarisation in $b \rightarrow s\gamma$ using the $B \rightarrow K^* e^+ e^-$ decay channel, LHCb 2009-008.
- [20] G. Raven, B physics results from the LHC, in: 25th International Symposium on Lepton Interactions at High Energies, Mumbai, India, August 2011, LHCb-TALK-2011-172.
- [21] CDF public note 10206 and D0 conference note 6093.
- [22] R. Fleischer, Nucl. Phys. B 671 (2003) 459.
- [23] A.J. Bevan, C. R. Physique 13 (2) (2012) 145–151.
- [24] A.I. Sanda, C. R. Physique 13 (2) (2012) 141–144.
- [25] P. Raimondi, et al., in: The Proceedings of the 11th European Particle Accelerator Conference (EPAC 08), Magazzini del Cotone, Genoa, Italy, 23–27 June 2008, pp WEXG02;
D. Alesini, et al., Nucl. Phys. Proc. Suppl. 181–182 (2008) 385;
C. Milardi, et al., Nuovo Cim. 32C (2009) 379.
- [26] M. Bona, et al., arXiv:0709.0451 [hep-ex];
D.G. Hitlin, et al., arXiv:0810.1312 [hep-ph];
T. Browder, M. Ciuchini, T. Gershon, M. Hazumi, T. Hurth, Y. Okada, A. Stocchi, JHEP 0802 (2008) 110, arXiv:0710.3799 [hep-ph];
A.G. Akeroyd, et al., SuperKEKB Physics Working Group, arXiv:hep-ex/0406071;
J.L. Hewett, et al., The discovery potential of a Super B factory, in: Proceedings, SLAC, arXiv:hep-ph/0503261.
- [27] D. Bečirević, V. Lubicz, C. R. Physique 13 (2) (2012) 121–126.
- [28] L.J. Hall, V.A. Kostelecky, S. Raby, Nucl. Phys. B 267 (1986) 415;
F. Gabbiani, E. Gabrielli, A. Masiero, L. Silvestrini, Nucl. Phys. B 477 (1996) 321, arXiv:hep-ph/9604387;
M. Ciuchini, E. Franco, A. Masiero, L. Silvestrini, Phys. Rev. D 67 (2003) 075016, arXiv:hep-ph/0212397;
M. Ciuchini, E. Franco, A. Masiero, L. Silvestrini, Phys. Rev. D 68 (2003) 079901 (Erratum).
- [29] M.A. Sanchis-Lozano, Int. J. Mod. Phys. A 19 (2004) 2183, arXiv:hep-ph/0307313;
E. Accomando, et al., arXiv:hep-ph/0608079;
M. Carena, J.R. Ellis, A. Pilaftsis, C.E.M. Wagner, Phys. Lett. B 495 (2000) 155, arXiv:hep-ph/0009212;
D. Besson, CLEO Collaboration, Phys. Rev. Lett. 98 (2007) 052002, arXiv:hep-ex/0607019;
J.F. Guionin, D. Hooper, B. McElrath, Phys. Rev. D 73 (2006) 015011, arXiv:hep-ph/0509024.
- [30] B. McElrath, Phys. Rev. D 72 (2005) 103508, arXiv:hep-ph/0506151.